Langmuir

Article

pubs.acs.org/Langmuir

Fabrication of Wafer-Size Monolayer Close-Packed Colloidal Crystals via Slope Self-Assembly and Thermal Treatment

Yizhi Wu, Cheng Zhang, Ye Yuan,† Ziwen Wang, Weijia Shao, Huijie Wang, and Xiaoliang Xu*

Department of Physics, University of Science and Technology of China, Hefei, Anhui 230026, China

Supporting Information

ABSTRACT: We developed a simple and general approach for constructing a wafer-scale monolayer, close-packed polystyrene (PS), and SiO_2 sphere arrays, namely colloidal crystals, which have significant potential in various applications. The method combines slope self-assembly and thermal treatment to achieve large-area and high-quality colloidal crystal with a proper slant angle (θ) and latex concentration (volume fraction, φ). The dependence of the structures of colloidal crystals on a dispersion system was also investigated. Moreover, a theoretical analysis of the slope self-assembly method was proposed. In addition, we applied the method to assemble PS spheres on different kinds of substrates, which indicates that the method is a versatile and reliable way to fabricate monolayer colloidal crystals.

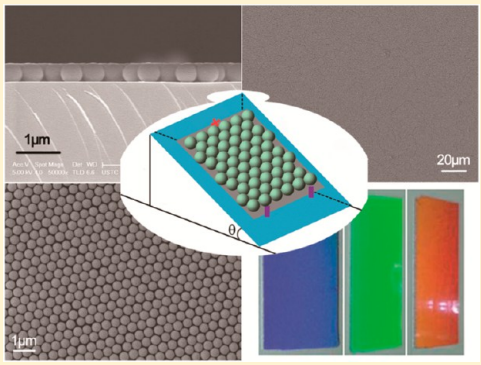

1. INTRODUCTION

Two-dimensional (2D) colloidal crystals have been attracting great attention in science and technology, as they have been applied in multiple fields including biosensors,[1] nanolithography,[2] and plasmonics.[3] In addition to the above applications, interests in this topic are also driven by the demand from data storage[4] and photonics[5] to meet the ever-growing necessity for improved performance and decreased cost. A variety of technologies, such as dip-coating,[6−8] spin-coating,[9] electric field assisted self-assembly,[10] defined area evaporation induced assembly,[11,12] and floating-transferring[13,14] methods, have been developed to create 2D colloidal crystals. All these techniques can be divided into two main categories: direct assembly on a solid substrate and liquid interface-mediated processes.[15,16] Direct assembly methods are experimentally more straightforward, not requiring any special instruments or artificial skill. The liquid interface-mediated processes possess the nature of the preassembly at an interface, and no precautions have to be taken to prevent the formation of multilayers.

The floating-transfer method is a commonly used interface-mediated approach[16] to achieve monolayer colloidal crystals, and it was first reported by Lenzamann and co-workers in 1993.[17] The method consists of two steps: first, slowly and steadily depositing a liquid dispersion of the spheres on a clean water surface using a syringe; second, transferring spheres to a target substrate. The resultant crystals contained a lot of defects, and a maximum area of 0.5 cm^2 monolayer arrays was obtained. The method was further improved by Burmeister's group[18] when they stabilized the colloidal monolayer by vacuum deposition of a metal or by thermal annealing before the transfer to circumvent the randomness of the crystallization process. Recently, Retsch et al.[19] further developed the method, namely by introducing a "parent substrate" and combining the adjustment of other parameter (like subphase pH and the addition of surfactants) to achieve close-packed colloidal 2D crystals with a large domain size. Very recently, Vogel's group[14] demonstrated the formation of binary colloidal monolayers at the air−water interface with precisely adjustable compositions over a wide range of size and number ratios using a Langmuir trough. However, the colloidal monolayer can be easily damaged when it is transferred to the target substrate from the interface of air/liquid, and this technique requires delicate precision skills.

The spin-coating and dip-coating are very simple direct assembly methods. Hulteen and Van Duyne[20] used a spin-coating procedure and, by varying the particle concentration and spin speed, could reproducibly fabricate single and double layers of PS spheres. However, this requires tight control over both experimental and ambient conditions, which can be demanding to regulate and cumbersome to optimize.[15] The approach of direct assembly most suitable for industrial applications is dip-coating,[21] which was first developed by Dimitrov et al.[22] In this approach, a glass plate is vertically dipped into a colloidal suspension and afterward very slowly withdrawn. The advantage of this method is that controlled and continuous growth of layered particle arrays on a large surface area can be realized. However, it is not widely used to obtain a colloidal monolayers because it is only capable of producing up to centimeter-sized, polycrystalline monolayer colloidal arrays, and the assembly rate in most cases is relatively slow.[23] We believe these drawbacks of dip-coating could be ascribed to two main factors. First, vibration is inevitable during the lifting-up

Received: October 23, 2012
Revised: September 21, 2013
Published: October 22, 2013

process, which usually leads to defects. And second, the low withdrawal rate, whose speed is equal to the arrays formation rate, is necessary to form large-size particle arrays and thus leads to low output. To sum up, these strategies are neither favorable for high output nor capable of building colloidal monolayers with single crystal characteristic. In addition, some of these methods seem infeasible due to tedious fabrication processes and incompatibility to wafer-scale bath microfabrications widely used by the semiconductor industry.

Inspired by the dip-coating method, we developed an alternative approach, namely a slope self-assembly method, to create large-size monolayer colloidal crystals. This method could potentially overcome the drawbacks mentioned above and texture the wafer-scale surface area with monolayer-hexagonal-closed PS spheres. There is little literature about PS spheres assembly of this kind. Micheletto and co-workers[24] deposited arrays of 42 nm sized latex spheres using a Peltier cell, whose system was tilted about 9°. It is the smallest regular monolayer array ever deposited, and areas of 0.5 cm^2 are covered by monolayers, whose hexagonal-close-packed areas were much smaller domains. Shortly thereafter, Rakers et al.[25] found well-ordered particle monofilms from polydisperse latex solutions could be more effectively created at the temperature of 2 °C, rather than 20 °C. To our best knowledge, there is no report using this method to achieve a large-area colloidal monolayer. We present a theoretical analysis that indicates an improved method based on drop-casting (namely slope self-assembly) which can achieve wafer-scale monolayer crystals. Our object is to establish a simple and versatile approach for constructing a wafer-scale colloidal monolayer which is compatible with the requirements of the semiconductor industry. We have found the proper dispersion media and thermal treatment are very important to achieve large-area colloidal crystals for slope self-assembly. Moreover, we have found that the "higher" temperature is preferred to transform the multilayer PS spheres into monolayers and thus to obtain high quality crystals, which is different from the results of Rakers's work. What is more, we find the latex film seems to become wet all the time and has a tendency to shrink down to latex drops when placed in a low temperature environment (such as 0 °C). Eventually, we obtained a wafer-scale (2 in. diameter) colloidal monolayer with few defects via the execution of varying the substrate slant angle under a determined liquid to particle concentration. In addition, we also investigated the self-assembly of PS spheres on different kinds of substrates, such as brass foils, silicon and silicon nitride, and the SiO_2 spheres slope self-assembly on silicon substrates, which indicates that the method we propose is versatile. The effect of ambient humidity and PS size on the optimum slope angle for the self-assembly are also discussed. What is more, we find this method is more tolerant than the spin-coating method for the roughness of the substrate to PS spheres self-assembly. It is worthwhile to mention here that our procedure is compatible with the requirements of the semiconductor industry. The method does not need to electrify the particles, and there is no confinement between any boundaries or surface pressure controls.

2. EXPERIMENTAL SECTION

Chemicals and Materials. The chemical reagents, such as styrene (≥99.0 wt %), sodium hydroxide (≥96.0 wt %), sodium dodecyl sulfate (CP grade), potassium peroxydisulfate (≥99.5 wt %), ethylene glycol (≥99.0 wt %), ethanol (≥99.5 wt %), and concentrated sulfuric acid (≥95.0 wt %), were used as received without further purification, after their purchase from Sinopharm Chemical Reagent Co., Ltd. (SCRC). The resistivity of the deionized water (DI water) is 18.25 MΩ·cm.

Silicon wafers were purchased from Lijing Optoelectronic Technologies Co. (Zhejiang). (3-Aminopropyl)triethoxysilane (98.0 wt %) and normal brass foils (alloy 260, 0.25 mm thick, 15 cm × 45 cm) were purchased from Alfa Aesar Co., Ltd. Brass foils with single side polishing were purchased from Tianlong Electronics Manufacturing Co. (Guangzhou). Silicon nitride substrates were prepared by deposition of silicon nitride onto silicon substrates using a plasma-enhanced chemical vapor system (PD-220, Samco Co., Ltd., Japan).

Wettability Treatment for All Kinds of Substrates. Silicon wafers were cut into 3 cm × 1.5 cm pieces, cleaned according to the RCA procedure,[26] and subsequently immersed in a piranha solution (70% H_2SO_4 + 30% H_2O_2) for 12 h, followed by triple rinsing in DI water. The surfaces of the brasses were coated with amino groups by dipping the slides in a 1% ethanol solution of (3-aminopropyl)-triethoxysilane for 6 h at room temperature. Silicon nitride substrates were soaked in concentrated sulfuric acid for 6 h, followed by triple rinsing in DI water. All the slides were air-dried.

Preparation of Colloidal Dispersions. PS latex was synthesized according to the method reported by Zhang et al.[27] The obtained polystyrene spheres were cleaned using successive centrifugation and ultrasonic cleaning in an ethanol system three times. Prior to use, the purified polystyrene spheres were redispersed in different solvents, such as ethanol, water, and a mixture of ethanol and glycol, and the final volume fraction was set to about 8%. For the dispersion system of ethylene glycol and ethanol (using a 1:1 mixture of ethylene glycol/ethanol), the volume fractions of 16%, 32%, and 40% were also prepared. For the dispersion system of water, the latexes of volume fractions of 16% and 28% were also prepared.

Silica spheres were synthesized according to Stober's processing.[28] The obtained SiO_2 spheres were cleaned using successive centrifugation and ultrasonic cleaning in an ethanol system three times. Prior to use, the purified polystyrene spheres were redispersed in a mixture of ethanol and glycol, and the final volume fraction was set to about 30%.

PS Spheres Slope Self-Assembly and Thermal Treatment. A certain volume of the above colloidal latex was deposited on substrates. To spread the solution to the full surface of the substrates, they were tilted at a variety of angles to the horizontal plane. And then some were dried at room temperature (25 °C), and others were dried in an oven set to 45 °C. The excess latex was wiped off the bottoms of the substrates.

PS Spheres Spin-Coating Self-Assembly. The next substrates were spin-coated at 550 rpm on a commercial spin coater (CAS, KW-4A) for 9 s to spread the PS latex, and then the substrates were quickly accelerated to 3500 rpm for 30 s. After spin-coating, the substrates were then transferred to an electric thermostatic drying oven with a quartz window until completely dried.

Structure Observation. The structure and morphology of the resultant colloidal crystals were examined by the field emission scanning electron microscope (SEM, JSM-6700F) operating at 5 kV.

3. RESULTS AND DISCUSSION

To quantify the ordering of the colloidal monolayer, we employ a well-established method, namely a two-dimensional discrete Fourier transform (DFT). We will briefly describe the principle of DFT, and the details can be seen in other literature.[29] For a perfect lattice composed of sharp bright spots, they can be approximated by an array of delta functions, $p(x)$. The spots composed of m elements separated in space by an interval T, we have

$$p(x) = \sum_{m=-\infty}^{\infty} \delta(x - mT)$$

dx.doi.org/10.1021/la402652t | Langmuir 2013, 29, 14017−14023

The corresponding FT harmonics are all of the same magnitudes described by

$$p(f) = \frac{1}{T}\sum_{n=-\infty}^{\infty}\delta(f - mT_f)$$

where $T_f = 1/T$. However, the magnitude of the harmonics in a disordered lattice decreases with the harmonic index. The apparently decreased rate of harmonic magnitudes points to a lower concentration of lattice defects. A typical assessment process of the colloidal monolayer can be seen in Supporting Information S1.

The diameter of the PS spheres we synthesized is 460 ± 20 nm. In our procedure, we discovered that the dispersion systems of both the ethanol and the water did not wet the silicon surfaces well. What is worse, the ethanol is volatile and the latex with the ethanol as a dispersion system dried too quickly after being dropped onto the silicon surface. Consequently, it is difficult to uniformly spread the latex onto the silicon surface within the drying process. To overcome this problem, we introduced an equal volume mixture of ethanol and glycol and achieved satisfying results. The topographies of the resultant samples were characterized by the SEM, and the results are shown in Figure 1. From Figure

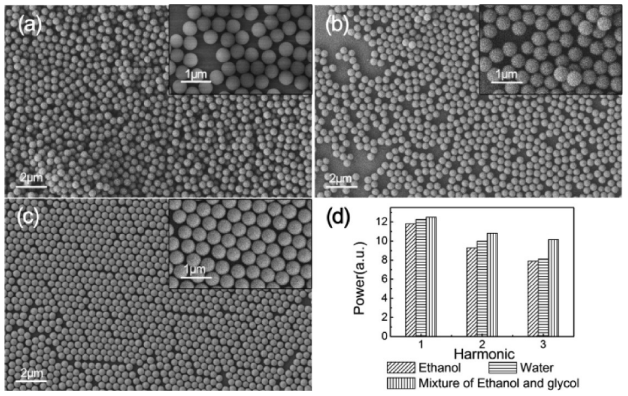

Figure 1. Different dispersion systems for PS spheres are (a) ethanol, (b) water, (c) a mixture of ethanol and glycol, and (d) the first three harmonic amplitudes of the power spectral density (PSD) of the FT images obtained from the SEM images (a)−(c). The concentration of the latex used in these experiments is φ = 8%, the slant angle is θ = 50°, and the self-assembly temperature is room temperature (25 °C).

1a, we can see that the colloidal array is multilayered and disordered, which is caused by the bad wetting characteristic of the substrate and the too rapid drying process of the latex with ethanol as a dispersion media. Figure 1b demonstrates that the ordering of the PS spheres array which used water as a dispersion media was greatly increased compared with the array formed from the dispersion media of ethanol. However, there are still multilayer PS spheres in some local small domains (inset of Figure 1b), and the PS spheres are packed in a loose way in some areas. Finally, the equal volume mixture of ethanol and glycol was introduced as a dispersion media. Figure 1c demonstrates that no multilayer PS spheres exist in the colloidal array using the ethanol and glycol mixture as the dispersion media, and the PS spheres are more closely packed compared to that using the other liquids as dispersion media. However, the disadvantage of the self-assembly using the mixture of ethanol and glycol as the dispersion media is its time-consuming nature, as half a day is needed to dry the liquid.

Figure 1d shows the amplitudes of the first three harmonics of the PSD of the FT images obtained from the SEM images (a)−(c). It suggests that the magnitude of the first harmonic of the PSD of the crystal using the mixture of the ethanol and glycol as the dispersion media (12.51) is the largest; namely, the ordering of the crystal is the best of the three kinds of dispersion systems. Consequently, we used the ethanol and glycol mixture as the dispersion media for the self-assembly of the PS spheres on silicon surfaces.

Figure 2 demonstrates how the PS spheres colloidal array varies as the slant angle of the slope increases. The magnitude

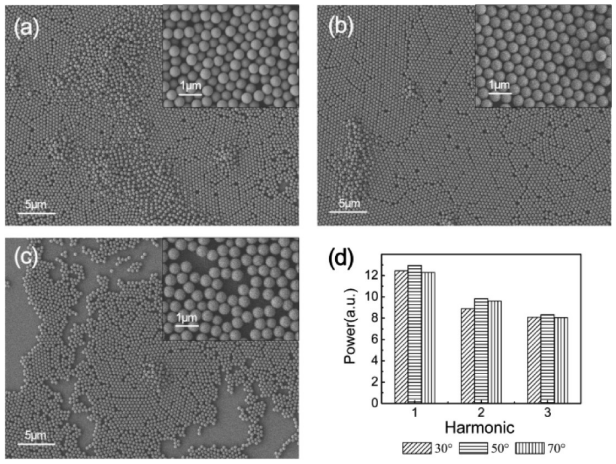

Figure 2. Different slant angles for PS self-assembly under the 25 °C environment with the latex concentration of φ = 32% using a mixture of ethanol and glycol as the dispersion media are (a) θ = 30°, (b) θ = 50°, (c) θ = 70° and (d) the amplitudes of the first three harmonics of the PSD of the FT images obtained from SEM images (a)−(c).

of the shear force (see Supporting Information S8) varies as the angle of the slope varies, and the shear force makes the latex spread over the surface of the silicon substrate. The latex was dropped onto the silicon substrate which was placed at an angle of approximately 30° with respect to the horizontal plane. The resultant array of PS spheres is seriously multilayered (Figure 2a). One explanation could be that the shear force is too small to spread the PS latex well over the surface of the substrate. It is reasonable that the area of multilayered PS spheres would decrease if the slant angle was increased, as the latex could flow more smoothly along the surface of the silicon (Figure 2b). Through mass experiments, we found 50 was an optimum slant angle, and the resultant colloidal array was of wafer scale. The colloidal array was mostly monolayer and close-packed except for some domains that had a few multilayers of PS spheres (Figure 2b and the inset). However, the lattice ordering of the colloidal crystal worsens (the inset of Figure 2c) when the slant angle is further increased. An interesting appearance also emerged, namely, a lot of vacancies are generated by the excess PS spheres latex running off the silicon surface. Figure 2d clearly shows the ordering of the crystal can be improved as the slope angle's increase, but with a contrary result when the slope angle exceeds 50°. Unfortunately, we still could not harvest a perfect monolayer, hexagonal, close-packed PS spheres array through simply changing the slant angle.

In the above section, we have mentioned that there are still a few multilayer PS spheres in some small domains under the concentration of φ = 32%. In this section, we will describe how we applied thermal treatments to obtain a monolayer array of

dx.doi.org/10.1021/la402652t | Langmuir 2013, 29, 14017−14023

PS spheres. As commonly known, when liquid is heated, Brownian motion will be enhanced and an effective stochastic force will be introduced. The remaining multilayer PS spheres could be scattered into a monolayer with the impact of the stochastic force. The microscopic images of the resultant colloidal crystal can be seen clearly in Figures 3a,b. Moreover,

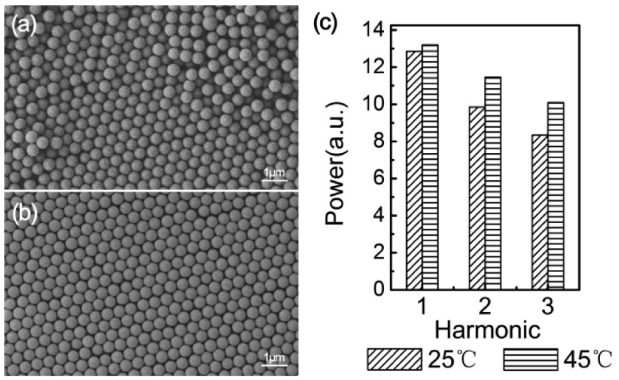

Figure 3. Typical top-view SEM images of (a) colloidal crystal A obtained under 25 °C, (b) colloidal crystal B obtained at 45 °C, both using a mixture of ethanol and glycol as the dispersion system, and (c) the amplitudes of the first three harmonics of the PSD of the FT images obtained from SEM images (a) and (b). Other conditions are the same: the PS latex concentration and the self-assembly slant angles are 32% and 50°, respectively.

by doing this, the self-assembly time decreased from half a day to 15 min due to the accelerated evaporation of the liquid, and the whole procedure took only half an hour. In addition, the powers (M) of all the FT harmonics (Figure 3c) are higher for the sample obtained under thermal treatment (45 °C), indicating a better regularity of its lattice. The apparently lower rate of harmonic magnitudes of the B sample points to a lower concentration of lattice defects in this sample. For example, the ratio M_1/M_2 reduces from 1.32 in the A sample to 1.15 in the B sample (Figure 3c). It is very clear that the thermal treatment improves the quality of the resultant colloidal crystal.

Different ambient humidity accompanies with the different temperatures. We detected the ambient humidity at 0, 25, and 45 °C (using the mixture of ethanol and glycol as dispersion media), and they are 76%, 39%, and 17%, respectively. The evaporation of solvent slow down when the ambient humidity increases, resulting in the worse colloidal crystal. However, too quick evaporation should be avoided, and the detailed reason will be discussed in the section of "theoretical analysis for slope self-assembly". Consequently, the proper ambient humidity is needed to achieve the good colloidal monolayer.

We investigated the effect of the concentration of the latex, and the results are shown in Figure 4. It shows that approximately half of the surface of the sample is covered with PS spheres when the concentration is φ = 8% (Figure 4a). And it is clear that the area covered by PS spheres grows larger as the latex concentration increases. The PS spheres covered the whole surface area at φ = 32% (Figure 4b), although multilayer PS spheres appear in some areas when the concentration exceeds φ = 32% (Figure 4c). Figure 4d indeed shows that the crystal which used the latex concentration of φ = 32% has the largest M value; namely, it has the largest area and fewest defects. It is worth mentioning here that the colloidal crystal obtained by this method is nearly defect-free (Figure 4b

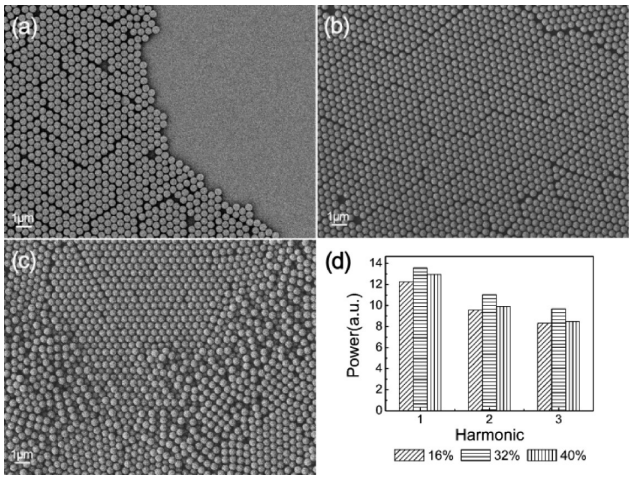

Figure 4. Different concentrations of PS latex: (a) φ = 16%, (b) φ = 32%, (c) φ = 40% and (d) the amplitudes of the first three harmonics of the PSD of the FT images obtained from the SEM images (a)−(c). Other conditions such as the self-assembly temperature (45 °C) and the slant angle (50°) are the same.

and table of contents graphic). In addition, we also achieved wafer-scale crystals, and the SEM images with low magnification and macrograph are shown in Figures S1a, S2, and S3. Up to this point, we have obtained the wafer-scale monolayer colloidal crystals with the latex concentration of φ = 32%, which used a mixture of ethanol and glycol as the dispersion media, under a 45 °C self-assembly environment and the 50° slant angle.

Herein, we propose a theoretical analysis for the mechanism of uniform spheres (such as PS spheres, SiO_2 spheres, etc.) slope self-assembly based on our procedure. For simplicity, we illustrate the PS spheres slope self-assembly and then indicate the analysis could also be applied to other kinds of spheres self-assembly. We analyze the major forces acting on the PS spheres and their effects on them. In addition, we discuss the effect of thermal treatment applying thermal dynamics and statistical physics. We propose that the slope self-assembly is virtually a phase transition process.

Through the force analysis of the PS spheres (see Supporting Information S7), we found that the major forces acting on the PS spheres include (1) fluid shear force (F_s), (2) gravity (G), and (3) capillary force (F_x). When the PS latex was first dripped onto the silicon surface, it flowed down and overspread the silicon surface rapidly, which took about 1.5 s. Thereafter, the flow velocity of the remaining liquid at the upper side of the silicon slowed down. We suppose a gradient of velocity perpendicular to the silicon surface exists in the liquid flow (Figure S4) and that naturally the resistance from the silicon surface and the PS spheres near the surface contribute to reducing the speed of the lower layer of the flow. Thus, the PS spheres on the upper side of the fluid move more quickly than the PS spheres on the lower side due to greater shear forces. Once the PS spheres on the upper side moved to positions where no other PS spheres were beneath them, they can move down onto the silicon surface in an approximate parabola trajectory under the effect of gravity (Figure 5b and Figure S4). And then, they slow down as a result of the shear forces becoming smaller (see Supporting Information S8), providing the possibility for other upper layer PS spheres to surpass them and fall ahead of them. In addition, gravity is greater than the

dx.doi.org/10.1021/la402652t | Langmuir 2013, 29, 14017−14023

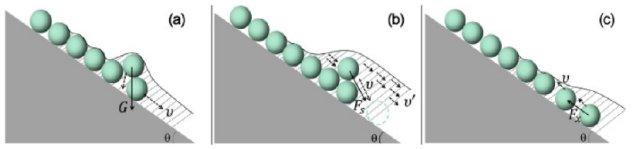

Figure 5. Mechanism for the uniform spheres slope self-assembly: (a) gravity force breaking up the multilayer spheres into monolayers; (b) shear force spreading the latex over the surface of the substrate and further breaking up the multilayer spheres into monolayers; and (c) capillary force close-packing the PS spheres.

buoyancy, providing a possible way that the upper layer spheres go directly to the lower layer space (Figure 5a). Therefore, fluid shear force and gravity both play a crucial role in causing the PS spheres to become a monolayer.

As evaporation proceeded, the PS latex dried from the top to the bottom on the silicon surface, leading to the formation of a nucleus zone of 2D crystals on the top. Capillary force acted on the PS spheres near the nucleus when the thickness of the concave layer of water became equal to the particle diameter,[30] and this pushed them toward the upper nucleus zone. The particles in the thicker layer began to move toward the upper zone, reaching the boundary of the arrays (Figure 5c), which was caused by convective transport. The mechanism of the slope self-assembly is similar to that on a horizontal hydrophilic glass plate reported by Denkov et al.[31] However, the difference is obvious because the drying process is directive for the slope self-assembly, namely along the downward slope, rather than randomly taking place anywhere on the silicon surface until all the dispersion media has evaporated. The advantage of the directionality of the slope self-assembly is in providing the possibility of producing defect-free and wafer-scale colloidal crystals. While the plane self-assembly for monolayer PS spheres will inevitably leave vacancies due to the randomness of the nucleus zones, theoretically, the slope self-assembly will totally overcome this shortcoming.

In view of thermal dynamics and statistical physics, slope self-assembly is a process of crystal formation and thus a phase transition. The PS latex is a dynamic system with multibody interactions, and the self-assembly is a complex process involving the effects of these interactions. Different phases would form under different thermodynamics conditions, but the direction of the phase transition will be toward a state with the minimum energy. The PS spheres will find the positions where they can form a state with minimum energy in the free energy landscape. For our samples consisting of hard PS spheres, the state with minimum free energy is a close-packed hexagonal monolayer. When the slope self-assembly process is at a lower temperature (room temperature), Brownian motion is weaker and the kinetic energy of a single PS sphere is low. Thus, the ability of PS spheres to search ergodically for the free energy landscape is poor. When the temperature increases, the kinetic energy of the PS spheres increases correspondingly, giving them a greater range of movement range, promoting their capability to search for the state with the lowest energy. That is the function of the thermal treatment on the slope self-assembly for constructing a better close-packed PS sphere monolayer. The thermal treatment seems to act in the role of noise acoustic vibration to some extent, which introduces "stochastic forces" to assist crystallization of opal films.[32] However, overly high temperatures should be avoided because the self-assembly needs a certain amount of time to achieve and overly high temperatures will make the liquid dry too quickly, leading to defective crystals. We should point out here that the above theoretical analysis can also be applied to other kinds of spheres, whose mass density is higher than the dispersion media, for self-assembly.

From the above analysis, we expect that this method may rely less on the smoothness standard of the substrate, while spin-coating usually requires a strictly smooth surfaces for assembling PS spheres. To confirm this, we investigated PS spheres slope self-assembly on brass foils with single side polishing, with rougher surface than silicon's. We also assembled the PS spheres on the same substrate using the spin-coating method. We have found that deionized water is more suitable for use as a dispersion media than a mixture of ethanol and glycol. Consequently, we dispersed PS spheres in deionized water for their self-assembly on brass. The slant angle is 40°, the self-assembly temperature is 40 °C, and the latex concentration is 16 vol %.

Figures 6a,b show the resultant crystals on brass foils. The PS spheres array obtained from spin-coating is packed in a random

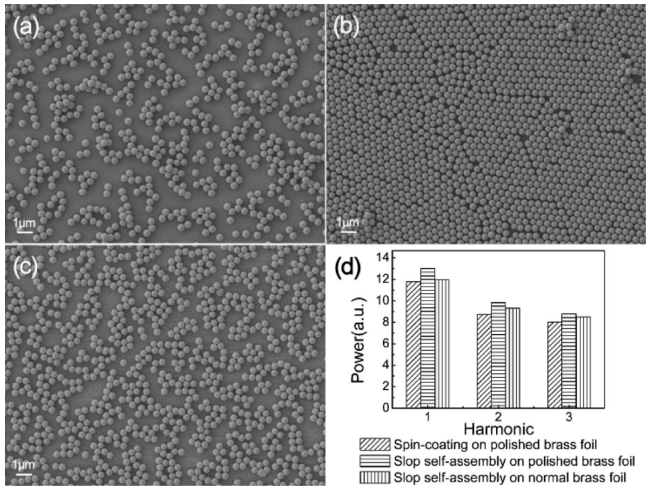

Figure 6. Roughness dependence for the self-assembly of PS spheres: (a) spin-coating on brass foils with single side polishing; (b) slope self-assembly on brass foils with single side polishing; (c) slope self-assembly on normal brass foils; and (d) the amplitudes of the first three harmonics of the PSD of the FT images obtained from SEM images (a)–(c).

and loose way (Figure 6a), whereas the ordering of the PS spheres array obtained from the slope-assembly is much better (Figure 6b). In the FT pattern of the large lattice areas (Figure 6d), the increase in the magnitudes of the first three harmonics are 1.23, 1.14 and 0.78, respectively. This means that, on average, the crystal obtained from the slope self-assembly results in an 11.08% improvement of the sphere lattice ordering over the spin-coating. This great improvement can be ascribed to the fact that the slope self-assembly can overcome the potential barriers of the brass foils more effectively than the spin-coating self-assembly. We believe that the slope assembly will also work well when there are stripe barriers on the substrate, such as finger electrodes on solar cells. However, if the barrier of the substrate is random and serious, the slope assembly will not work well (Figure 6c). In other words, the slope assembly still requires a fairly smooth surface.

Slope self-assembly is a versatile method for achieving large-area colloidal crystals. Figure 7a shows a colloidal monolayer which was obtained on a silicon nitrides layer (which is often

dx.doi.org/10.1021/la402652t | Langmuir 2013, 29, 14017−14023

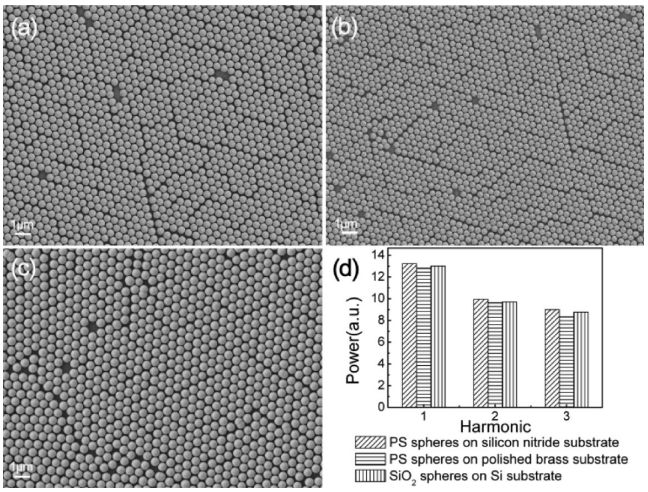

Figure 7. Versatile slope self-assembly: (a) silicon nitride substrate; (b) brass foils with single side polishing; (c) SiO_2 spheres self-assembly on silicon substrate, and (d) the amplitudes of the first three harmonics of the PSD of the FT images obtained from SEM images (a)−(c).

used as an antireflection layer on the top of solar cells). The resultant colloidal monolayer is quite good and could be comparable to the crystals we obtained on the silicon surfaces. The self-assembly conditions are a slant angle of 50°, a self-assembly temperature of 45 °C, and the latex concentration of 32 vol %, using a mixture of ethanol and glycol as the dispersion media. Figure 7b shows the large area crystal obtained from the surface of the brass foil with single side polishing, with self-assembly conditions of a slant angle of 50°, an assembly temperature of 43 °C, and a latex concentration of 28 vol %, using deionized water as the dispersion media. Although there are a little more defects than in the crystal obtained on silicon surface (Figure 7d), it may still have valuable applications. Moreover, we have also investigated the slope self-assembly of other kinds of spheres. Figure 7c shows SiO_2 spheres (with the diameter of 554 ± 12 nm) slope self-assembly on a silicon substrate. The resultant crystal is not as close-packed as the PS crystal obtained from a silicon surface, but it is actually "quasi-perfect", with very good crystal lattices. This reveals that the slope assembly can also be applied to the self-assembly of "heavy" spheres. The self-assembly conditions for SiO_2 spheres are a slant angle of 45°, a self-assembly temperature of 45 °C, and a latex concentration of 30 vol %, using the a mixture of ethanol and glycol as the dispersion media.

In addition, from Figure 4b, Figure 7c, and Figure S5, we can conclude that as the diameter of the sphere increases, the gravity increases and it promotes the ability of overspreading the latex onto the silicon surface. Hence, the optimum slope angle for self-assembly decreases when the size of spheres increase. For the self-assembly of 3 μm PS spheres (Figure S6), the resultant arrays is bad, which is caused by the increasing the adhesion force of the colloid sphere.

4. CONCLUSIONS

In summary, 2D monolayer hexagonal close-packed PS and SiO_2 spheres at the wafer-scale have been fabricated using slope self-assembly. By adjusting the slant angle and latex concentration under thermal treatment, we achieved nearly crack-free and wafer-scale colloidal crystals. And we also obtained a large-area PS spheres crystal on the surface of brass, silicon and silicon nitride, which shows the versatility of this method. In addition, we developed a theoretical analysis of our improved assembly method, suggesting that it could be a promising way to assemble PS spheres of other diameters and could also be used for the fabrication of colloidal crystals made from other kinds of spheres. Moreover, we discussed the effect of ambient humidity and PS size on the optimum slope angle for the self-assembly. What is more, this approach is not only time-saving but also highly compatible with contemporary microfabrication, which may accomplish the eventual mass production of low-cost practical devices, including data storage, nanolithography and plasmonics.

■ ASSOCIATED CONTENT

Supporting Information

Typical assessment process of the colloidal monolayer; SEM images and macroscopic graphics of the crystal obtained under optimized conditions; force analysis of a PS sphere; parameters of polystyrene spheres and dispersion systems. This material is available free of charge via the Internet at http://pubs.acs.org.

■ AUTHOR INFORMATION

Corresponding Author

*E-mail xlxu@ustc.edu.cn (X.X.).

Present Address

†Y.Y.: Department of Physics, University of Colorado, Boulder.

Notes

The authors declare no competing financial interest.

■ ACKNOWLEDGMENTS

We gratefully acknowledge the useful discussions and advice on the theoretical analysis of the slope self-assembly from Prof. Ning Xu, who comes from CAS Key Laboratory of Soft Matter Chemistry, University of Science and Technology of China, Hefei, People's Republic of China. We also thank so much Miss Sherri Nelson and Mr. Fred Firstbrook (for their careful proofreading and their enthusiastic support of this work), who both come from America and are currently teachers of University of Science and Technology of China. This work is supported by the National Natural Science Foundation of China under Grants 81172082 and 51272246.

■ ABBREVIATIONS

θ, slant angle; φ, volume fraction; 2D, two-dimensional; PS spheres, polystyrene spheres; DI water, deionized water; FESEM, field emission scanning electron microscopy; PSD, power spectral density; M, powers; DFT, discrete Fourier transform.

■ REFERENCES

(1) Baksh, M. M.; Jaros, M.; Groves, J. T. Detection of molecular interactions at membrane surfaces through colloid phase transitions. *Nature* **2004**, *427* (6970), 139−141.

(2) Zhang, J. H.; Li, Y. F.; Zhang, X. M.; Yang, B. Colloidal self-assembly meets nanofabrication: From two-dimensional colloidal crystals to nanostructure arrays. *Adv. Mater.* **2010**, *22* (38), 4249−4269.

(3) Vogel, N.; Jung, M.; Bocchio, N. L.; Retsch, M.; Kreiter, M.; Koper, I. Reusable localized surface plasmon sensors based on ultrastable nanostructures. *Small* **2010**, *6* (1), 104−109.

(4) Sun, S. H.; Murray, C. B.; Weller, D.; Folks, L.; Moser, A. Monodisperse FePt nanoparticles and ferromagnetic FePt nanocrystal superlattices. *Science* **2000**, *287* (5460), 1989−1992.

(5) Marlow, F.; Muldarisnur; Sharifi, P.; Brinkmann, R.; Mendive, C. Opals: status and prospects. *Angew. Chem., Int. Ed.* **2009**, *48* (34), 6212−6233.
(6) Li, X.; Wang, T. Q.; Zhang, J. H.; Yan, X.; Zhang, X. M.; Zhu, D. F.; Li, W.; Zhang, X.; Yang, B. Modulating two-dimensional non-close-packed colloidal crystal arrays by deformable soft lithography. *Langmuir* **2010**, *26* (4), 2930−2936.
(7) Hatton, B.; Mishchenko, L.; Davis, S.; Sandhage, K. H.; Aizenberg, J. Assembly of large-area, highly ordered, crack-free inverse opal films. *Proc. Natl. Acad. Sci. U. S. A.* **2010**, *107* (23), 10354−10359.
(8) Tan, K. W.; Saba, S. A.; Arora, H.; Thompson, M. O.; Wiesner, U. Colloidal self-assembly-directed laser-induced non-close-packed crystalline silicon nanostructures. *ACS Nano* **2011**, *5* (10), 7960−7966.
(9) Lu, Z. X.; Namboodiri, A.; Collinson, M. M. Self-supporting nanopore membranes with controlled pore size and shape. *ACS Nano* **2008**, *2* (5), 993−999.
(10) Huang, X. G.; Zhou, J.; Fu, M.; Li, B.; Wang, Y. H.; Zhao, Q.; Yang, Z. W.; Xie, Q.; Li, L. T. Binary colloidal crystals with a wide range of size ratios via template-assisted electric-field-induced assembly. *Langmuir* **2007**, *23* (17), 8695−8698.
(11) Singh, G.; Gohri, V.; Pillai, S.; Arpanaei, A.; Foss, M.; Kingshott, P. Large-area protein patterns generated by ordered binary colloidal assemblies as templates. *ACS Nano* **2011**, *5* (5), 3542−3551.
(12) Singh, G.; Pillai, S.; Arpanaei, A.; Kingshott, P. Layer-by-layer growth of multicomponent colloidal crystals over large areas. *Adv. Funct. Mater.* **2011**, *21* (13), 2556−2563.
(13) Ctistis, G.; Patoka, P.; Wang, X.; Kempa, K.; Giersig, M. Optical transmission through hexagonal arrays of subwavelength holes in thin metal films. *Nano Lett.* **2007**, *7* (9), 2926−2930.
(14) Vogel, N.; de Viguerie, L.; Jonas, U.; Weiss, C. K.; Landfester, K. Wafer-scale fabrication of ordered binary colloidal monolayers with adjustable stoichiometries. *Adv. Funct. Mater.* **2011**, *21* (16), 3064−3073.
(15) Vogel, N.; Weiss, C. K.; Landfester, K. From soft to hard: the generation of functional and complex colloidal monolayers for nanolithography. *Soft Matter* **2012**, *8* (15), 4044−4061.
(16) McGorty, R.; Fung, J.; Kaz, D.; Manoharan, V. N. Colloidal self-assembly at an interface. *Mater. Today* **2010**, *13* (6), 34−42.
(17) Lenzmann, F.; Li, K.; Kitai, A. H.; Stover, H. D. H. Thin-film micropatterning using polymer microspheres. *Chem. Mater.* **1994**, *6* (2), 156−159.
(18) Burmeister, F.; Schäfle, C.; Matthes, T.; Böhmisch, M.; Boneberg, J.; Leiderer, P. Colloid monolayers as versatile lithographic masks. *Langmuir* **1997**, *13* (11), 2983−2987.
(19) Retsch, M.; Zhou, Z. C.; Rivera, S.; Kappl, M.; Zhao, X. S.; Jonas, U.; Li, Q. Fabrication of large-area, transferable colloidal monolayers utilizing self-assembly at the air/water interface. *Macromol. Chem. Phys.* **2009**, *210* (3−4), 230−241.
(20) Hulteen, J. C.; Vanduyne, R. P. Nanosphere lithography - A materials general fabrication process for periodic particle array surfaces. *J. Vac. Sci. Technol., A* **1995**, *13* (3), 1553−1558.
(21) Burmeister, F.; Schafle, C.; Keilhofer, B.; Bechinger, C.; Boneberg, J.; Leiderer, P. From mesoscopic to nanoscopic surface structures: Lithography with colloid monolayers. *Adv. Mater.* **1998**, *10* (6), 495-+.
(22) Dimitrov, A. S.; Nagayama, K. Continuous convective assembling of fine particles into two-dimensional arrays on solid surfaces. *Langmuir* **1996**, *12* (5), 1303−1311.
(23) Ye, X. Z.; Qi, L. M. Two-dimensionally patterned nanostructures based on monolayer colloidal crystals: Controllable fabrication, assembly, and applications. *Nano Today* **2011**, *6* (6), 608−631.
(24) Micheletto, R.; Fukuda, H.; Ohtsu, M. A simple method for the production of a two-dimensional, ordered array of small latex particles. *Langmuir* **1995**, *11* (9), 3333−3336.
(25) Rakers, S.; Chi, L. F.; Fuchs, H. Influence of the evaporation rate on the packing order of polydisperse latex monofilms. *Langmuir* **1997**, *13* (26), 7121−7124.
(26) Skidmore, K. Cleaning techniques for wafer surfaces. *Semicond. Int.* **1987**, *10* (9), 80−5.
(27) Zhang, J. H.; Chen, Z.; Wang, Z. L.; Zhang, W. Y.; Ming, N. B. Preparation of mohodisperse polystyrene spheres in aqueous alcohol system. *Mater. Lett.* **2003**, *57* (28), 4466−4470.
(28) Stober, W.; Fink, A.; Bohn, E. Controlled growth of monodisperse silica spheres in the micron size range. 1. *J. Colloid Interface Sci.* **1968**, *26* (1), 62−69.
(29) Khunsin, W.; Kocher, G.; Romanov, S. G.; Torres, C. M. S. Quantitative analysis of lattice ordering in thin film opal-based photonic crystals. *Adv. Funct. Mater.* **2008**, *18* (17), 2471−2479.
(30) Kralchevsky, P. A.; Nagayama, K. Capillary forces between colloidal particles. *Langmuir* **1994**, *10* (1), 23−36.
(31) Denkov, N. D.; Velev, O. D.; Kralchevsky, P. A.; Ivanov, I. B.; Yoshimura, H.; Nagayama, K. 2-Dimensional crystallization. *Nature* **1993**, *361* (6407), 26−26.
(32) Khunsin, W.; Amann, A.; Kocher-Oberlehner, G.; Romanov, S. G.; Pullteap, S.; Seat, H. C.; O'Reilly, E. P.; Zentel, R.; Torres, C. M. S. Noise-assisted crystallization of opal films. *Adv. Funct. Mater.* **2012**, *22* (9), 1812−1821.